Available online at www.sciencedirect.com
ScienceDirect
Acta Materialia 56 (2008) 802–808
Acta MATERIALIA
www.elsevier.com/locate/actamat

Enhancement of deformation of Ni–Mn–Ga martensite by dynamic loading

V.A. L'vov *, S. Kustov, E. Cesari

Universitat de les Illes Balears, Dept. de Física, Ctra. de Valldemossa km 7.5, E-07122, Palma de Mallorca, Spain

Received 18 July 2007; received in revised form 11 October 2007; accepted 16 October 2007
Available online 11 December 2007

Abstract

The process of deformation of twinned ferromagnetic martensite under a combined action of slowly increasing magnetic field (or mechanical stress) and oscillatory mechanical stress has been studied theoretically in the framework of a statistical model of magnetically/mechanically induced deformation. The dependencies of magnetically/mechanically induced deformation on time, oscillatory stress amplitude and magnetic field (or mechanical stress) has been modeled. The additional deformation of a Ni–Mn–Ga specimen activated by a superimposed oscillatory stress has been computed for the case of resonant longitudinal ultrasonic waves with several realistic values of strain amplitudes using the typical values of Young's modulus, specimen length, and threshold field/stress (i.e. the field/stress, which triggers the process of magnetically/mechanically induced deformation). Quantitative estimations show, in particular, that the ultrasonic wave with a strain amplitude of 4×10^{-5} causes a ~30% decrease of the threshold field/stress value; the additional deformation induced by the ultrasound reaches its maximal value ≈2.8% when the field/stress reaches the initial (i.e. observed in the absence of ultrasound) threshold value.
© 2007 Acta Materialia Inc. Published by Elsevier Ltd. All rights reserved.

Keywords: Ferromagnetic martensite; Ni–Mn–Ga; Ultrasound; Deformation

1. Introduction

Magnetic, elastic and magnetoelastic properties of Ni–Mn–Ga ferromagnetic shape memory alloys (FSMA) have attracted the attention of researchers during the last decade (see e.g. Refs. [1–5] and references therein). Detailed reviews of experimental and theoretical researches concerning the Ni–Mn–Ga alloy system are presented in Refs. [6,7]. The large values (>5%) of mechanically and magnetically induced deformations (MIDs) of these alloys achieved at unusually low compressive stresses (~2 MPa) [3,8] or moderate magnetic fields ($\mu_0 H \sim 0.5$–1.0 T) [2] are of a special interest. The large deformation of twinned Ni–Mn–Ga specimen originates from the mechanically/magnetically induced stressing/straining, which triggers a process of modification of twin structure above certain threshold stress/strain or field value; for more details see e.g. Refs. [2,3,7–10].

Since Ni–Mn–Ga alloys are used now for designing of magneto-mechanical actuators and sensors [11,12], lowering of threshold magnetic field and improvement of the dynamic properties of the devices based on MID are considered as challenging problems [13,14]. As far as the possibility of magnetic control of the MID is restricted by the value of magnetoelastic constant of a crystal [15], any non-magnetic mechanism enhancing the MID effect is of a great interest. Acoustic oscillations promote pseudoplastic deformation of shape memory alloys in the martensitic state, which proceeds through the reorientation of martensitic variants [16], and facilitate the stress-induced martensitic transformation [17]. These phenomena are manifestations of the acoustoplastic or Blaha effect, which is known for the conventional dislocation plasticity of crystals (see e.g.

* Corresponding author. Permanent address: Taras Shevchenko University, Radiophysics Department, Glushkov Street 2, Building 5, Kiev 03022, Ukraine.
E-mail address: victorlvov@univ.kiev.ua (V.A. L'vov).

1359-6454/$30.00 © 2007 Acta Materialia Inc. Published by Elsevier Ltd. All rights reserved.
doi:10.1016/j.actamat.2007.10.028

the review in Ref. [18] and references therein). Several interpretations of the acoustoplastic effect have been suggested, essentially based on the stress [19] or energy superposition principles [20]. Recently, a strong effect of superposition of sub-resonant mechanical oscillations on the MID has been reported for a Ni–Mn–Ga alloy [13], and an attempt has been undertaken to describe on a microscopic level the dynamics of an isolated martensitic twin boundary subjected to both external magnetic field and acoustic excitation [21].

The present work is aimed at theoretical description and quantitative estimation of the effect of oscillatory strain on the deformation of twinned ferromagnetic martensites in terms of macroscopic physical parameters, which are commonly used for the description of large MID. To this end a stress superposition principle is taken into account. Attention is focused on the resonant acoustic oscillations, but the developed theoretical model is fully applicable to the sub-resonant case. Numerical estimations of basic parameters characterizing MID are made for a twinned Ni–Mn–Ga single crystalline specimen with dimensions of $\sim 10^{-2}$ m, subjected to the effect of resonant oscillations at a frequency of around 10^5 Hz.

2. Statistical model of deformation of twinned martensite: generalization for superposition of oscillatory stress

The deformation of twinned Ni–Mn–Ga martensite can be described in the framework of a statistical model [22,23], which is based on the following assumptions: (i) the martensitic structure can be modeled by two alternating variants of tetragonal lattice with the principal axes [1 0 0] and [0 1 0] aligned with x and y directions, the neighboring variants form xy twins; (ii) the deformation of xy twin structure can be induced by the axial compression or magnetic field application; the applied force/field along x or y direction, see Fig. 1, creates an effective elastic/magnetoelastic stress $\sigma \equiv \sigma_{xx} - \sigma_{yy}$; (iii) the effective stress produces an elastic strain $\varepsilon^{\rm el} \equiv \varepsilon^{\rm el}_{xx} - \varepsilon^{\rm el}_{yy}$, which breaks the crystallographic equivalence of neighboring variants of the crystal lattice and causes jump-like displacements of twin boundaries; (iv) the effective stress fluctuates around a certain average value due to the thermal vibrations of crystal lattice; (v) the jumps of different twin boundaries occur in different moments $t(n)$, when the fluctuating effective stress crosses some critical levels $\sigma_n \equiv (\sigma_{xx} - \sigma_{yy})_n$ enumerated in ascending order; (vi) the twin boundaries jumps result in large deformations $\varepsilon \gg \varepsilon^{\rm el}$.

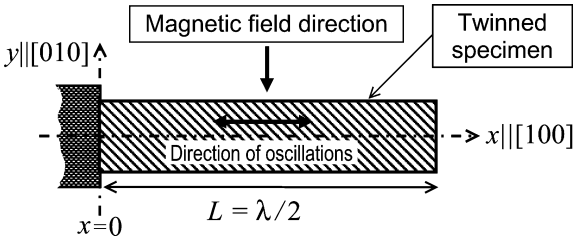

Fig. 1. Rod-shaped internally twinned specimen with the left end joined to an ultrasonic transducer. The length of the specimen is equal to the half-wavelength ($\lambda/2$) of the fundamental harmonic of longitudinal oscillations; hatching illustrates the orientation of twin boundaries.

Let the quasistatic magnetic field or compressive force be applied in the moment $t = 0$ to a twinned tetragonal martensite with $c/a < 1$ (c, a are the lattice parameters) in y direction and the uniaxial alternating mechanical stress

$$\tilde{\sigma} \equiv \tilde{\sigma}_{xx} = \sigma_{\rm A} \cos \omega t \tag{1}$$

with the amplitude $\sigma_{\rm A}$ and angular frequency ω, being superimposed on the quasistatic one $\sigma = \sigma_{yy}$ (see Fig. 1). In this case the total effective stress is the sum of the applied stress σ, random thermal stress $\xi(t)$ and alternating stress $\tilde{\sigma}$:

$$\sigma_t = \sigma + \xi(t) + \tilde{\sigma}. \tag{2}$$

It is convenient to simplify the model and substitute the alternating mechanical stress Eq. (1) by a sequence of rectangular pulses with the same frequency and with the same root-mean-square value of amplitude

$$\Delta_\pm = \pm \sigma_{\rm A}/\sqrt{2}. \tag{3}$$

This simplification is justified when the average attempt frequency of the stochastic crossings of critical levels by the total stress is substantially higher than ω, and this condition will be verified below. Eq. (3) implies that the average elastic energies of rectangular pulses and of the harmonic oscillation Eq. (1) are equal. Thus, the total effective stress is expressed by the formulae

$$\sigma_t = \sigma_\pm + \xi(t), \quad \sigma_\pm \equiv \sigma + \Delta_\pm. \tag{4}$$

For the crystal compressed in y direction the stress component σ_{yy} is negative, therefore $\sigma > 0$ and positive stress pulses promote deformation, which is induced by the magnetic field or compressive force, but the negative ones retard it. Due to this fact, the expected time interval before the first crossing of the nth stress level depends on the sign of stress pulse. According to Ref. [23] this interval is

$$\langle t_\pm(n) \rangle = \begin{cases} 0 & \text{if } \sigma_n < \sigma_\pm, \\ t_{\rm sw} + [v f_\pm(\sigma_n)]^{-1} & \text{if } \sigma_n \geqslant \sigma_\pm, \end{cases} \tag{5}$$

where

$$f_\pm(\sigma_n) = (\xi_0 \sqrt{2\pi})^{-1} \exp\{-(\sigma_n - \sigma_\pm)^2/2\xi_0^2\} \tag{6}$$

is the probability density of crossing of the nth level, $t_{\rm sw}$ is the time interval before the switching on mechanical oscillations, ξ_0 and v are the mean-square value and the average variation rate of random stress, respectively. Following Ref. [27]

$$\xi_0^2 = \frac{16\pi}{15} \cdot \frac{k_{\rm B} T C'}{\lambda_0^3}, \quad v(T) = \left(\frac{12C'}{5\rho}\right)^{1/2} \cdot \frac{\xi_0}{\lambda_0}, \tag{7}$$

where $C' = (C_{11} - C_{12})/2$ is the shear elastic modulus, λ_0 is a characteristic length scale of the order of twice the twin width (for more details see also Ref. [24]).

The values $t_\pm^{-1}$ are proportional to the probability densities of crossings of critical stress levels during the positive

and negative half-cycles of stress pulses. On average, the probability density is proportional to $(t_+^{-1}+t_-^{-1})/2$, and hence, in the presence of oscillations the expected time is expressed as

$$\langle t(n)\rangle = \begin{cases} t_+(n)|_{\varepsilon_A=0} = t_-(n)|_{\varepsilon_A=0} & \text{if } n < n_0, \\ t_{sw} + \frac{2t_+(n)t_-(n)}{t_+(n)+t_-(n)} - \frac{2t_+(n_0)t_-(n_0)}{t_+(n_0)+t_-(n_0)} & \text{if } n \geqslant n_0, \end{cases} \quad (8)$$

where n_0 is the number of levels crossed before switching on the oscillations.

The rest of the model equations are derived in Refs. [22,23]. The number of twin boundaries displaced during the time from $t=0$ to $t=\langle t(n)\rangle$ is

$$N(n) = N_0 \sum_j p(\sigma_j)\theta(\sigma_n - \sigma_j), \quad j = 1, 2, \ldots N_0, \quad (9)$$

where N_0 is the total number of critical stress levels, j enumerates these levels, θ is the stepwise Heaviside function,

$$p(\sigma_j) \propto \theta(\sigma - \sigma_c)\exp\{-(\sigma_j - \sigma_c)/2\sigma_0^2\} \quad (10)$$

is a phenomenological probability density distribution for the twin boundaries jumps. The Heaviside function is introduced in Eq. (10) to account for the threshold nature of the detwinning process (the condition $\sigma_t = \sigma_c$ corresponds to the start of this process). The volume fraction of y-variant of martensite, $\alpha_y(n)$, depends on the number n as follows:

$$\alpha_y(n) = \alpha_y(0) + [\alpha_y(N_0) - \alpha_y(0)]N(n)/N_0. \quad (11)$$

The alloy deformation in x direction satisfies the equation

$$\varepsilon(n) = \frac{1}{2E}\sigma + (1 - c/a)[\alpha_y(n) - \alpha_y(0)], \quad (12)$$

where E is Young's modulus.

Eqs. (3)–(12) constitute the background for the theoretical description of the deformation of twinned martensite under the combined action of slowly varying magnetic field/mechanical stress and mechanical oscillations. The resonant oscillations of the specimen can be incorporated in this description in a simple way. The periodic displacement in the longitudinal standing wave generated in a rod of length L (see Fig. 1) can be formulated in the continuum limit as

$$\tilde{u}_x = u_A \cos(\pi m x/L)\cos\omega t \quad (13)$$

where u_A is the displacement amplitude, $\omega = (E/\rho)^{1/2}(\pi m/L)$ is the resonance angular frequency of the specimen with the free-moving ends, $m = 1, 2, 3, \ldots$, and ρ is the mass density of the rod. Fig. 1 shows an example of such experimental arrangement when one of the rod ends is joined to an ultrasonic transducer and the second one is moving freely under the resonance conditions. If the rod is long enough, $L \gtrsim 10l$, where l is the dimension of the rod in y and z directions, only the displacement in x direction can be considered. The ε_{xx} strain tensor component is

$$\tilde{\varepsilon}_{xx} = -\varepsilon_A \sin(\pi m x/L)\cos\omega t, \quad (14)$$

where $\varepsilon_A = \pi m u_A/L$ is the strain amplitude.

As the simplest approach, the spatial distribution of strain in the standing wave can be replaced by the spatially uniform root-mean-square value of strain along the sample, which provides the same elastic energy as the strain in Eq. (14). This average strain is $(\varepsilon_A/\sqrt{2})\cos\omega t$ and for the case of resonant oscillations Eq. (3) yields $\Delta_\pm = \pm E\varepsilon_A/2$.

3. Results and discussion

The computations have been performed for ultrasonic standing wave conditions, since this allows one to approach the typical dimensions of samples ($L \approx 1$ cm) and realistic values of the oscillatory strain amplitude used in experiments, $\varepsilon_A \sim 10^{-6} - 10^{-4}$, which are known to promote pseudoplastic deformation of martensites and stress-induced martensitic transformation [16,17]. The modeling refers to the temperature of 290 K.

To begin with, it is useful to estimate basic parameters involved in the modeling, like magnitudes of thermal and oscillatory stress and the attempt frequency. Some relevant characteristics reported for Ni–Mn–Ga alloys by different authors as well as phenomenological parameters involved in the probability density distribution Eq. (10) are listed in Table 1. The experimental value of Young's modulus ($E \approx 3C' \approx 24$ GPa, see Table 1) and the amplitude of the oscillatory strain $\varepsilon_A = 4\times10^{-5}$ yield the oscillatory stress amplitude $\Delta_\pm = 0.5$ MPa.

The mean-square value of the random stress effectively interacting with the twin structure strongly depends on the twin width (see Ref. [24] and references therein). Hierarchic twin structure in Ni–Mn–Ga alloys and superfine twins with width ~100 nm are observed inside the twins of the micrometer scale (see e.g. Refs. [4,27]). For the 100 nm twins the mean-square value of the random stress ($\xi_0 \approx 0.5$ MPa, [24]) is close to the oscillatory stress estimated above. It is well established that the magnetic field application is equivalent to the mechanical stress in twinned ferromagnetic martensites [15,28]. The dependence

Table 1
Typical values of characteristics of Ni–Mn–Ga twinned martensite used in computations

Tetragonality of the lattice, c/a	Shear plastic modulus, C' (GPa)	Young's modulus, E	Mass density, ρ (g/cm^3)	Characteristic length scale[a] λ_0 (nm)	σ_c[b] (MPa)	σ_0[b]	Initial volume fraction of martensite, $\alpha_y(0)$
0.94 [25]	8 [26]	$3C'$	8.4	100 [4,27]	3.2	$\sigma_c/5$	0.05

[a] Of the order of twice the width of internal twins of martensitic variants.
[b] Parameters of the probability density distribution of the jumps of twin boundaries (see Eq. (10)).

of the equivalent stress on the magnetic field has been determined in Ref. [8] and is presented in Fig. 2. This figure shows that the saturating field induces the stress of about 3 MPa and that the effect of the oscillatory/thermal stress of ~0.5 MPa is equivalent to application of the magnetic field of about 0.2 T, being much lower than the saturating field. Since all stresses relevant to the problem under consideration do not exceed 3 MPa, classical plastic deformation has to be disregarded.

The average attempt frequency of stochastic crossing the critical stress levels can be estimated from the parameters of fluctuating thermal stress as $v/2\xi_0$. Using Eq. (7) and numerical values of C' and λ_0 from Table 1, one obtains $v/2\xi_0 \approx 7.5$ GHz. The average attempt frequency of crossing the critical stress levels can also be roughly estimated as $s_t/\lambda_0 \approx 10$ GHz, where $s_t = (C'/\rho)^{1/2}$ is the transversal sound velocity. This is an upper limit, which corresponds to the frequency of the shortest waves effectively interacting with the twin structure (for more details see Refs. [23,24,27]). These estimations show that the attempt frequency is substantially higher than a typical value of the frequency of the fundamental longitudinal resonance $\omega/2\pi = (E/\rho)^{1/2}/2L \approx 85$ kHz. Therefore, the simplification of the model introduced by Eq. (3) is well justified.

Let the stress σ increases in a stepwise manner with stress and time intervals $\Delta\sigma = 0.2$ MPa and $\Delta t = 20$ s (see Fig. 2). In this case Eqs. (3)–(12) enable the computation of dependencies of deformation on time and stress before and after switching on the oscillations. Then, the deformation–field dependencies can be plotted using the equivalent stress function $\sigma_{eq}(H)$, which has been determined in Ref. [8] from the series of experimental superelastic loops measured under different values of applied magnetic field. The graph of this function (solid line in Fig. 2) permits the transformation of deformation–stress curves into the deformation–field ones. The phenomenological parameters σ_c, σ_0 and $\alpha_y(0)$ (see Table 1) have been adjusted so as to achieve a good similarity between the theoretical stress–deformation curve and the experimental curve, which was used in Ref. [8] for the determination of equivalent stress function. The correspondence between theoretical and experimental stress–deformation dependencies is illustrated in Fig. 3.

The role of the ultrasonic oscillations in the deformation of twinned martensite is demonstrated in Fig. 4: the ultrasound with a strain amplitude of 2×10^{-5}, which was switched on in the moment $t_{sw} = 110$ s, reduces the expected times for crossing the critical stress levels and hence promotes the deformation of twinned martensite.

Fig. 5 shows the time evolution of deformation under a stepwise stress. For 0.7 MPa stress the deformation is elastic and cannot be discerned on the scale of Fig. 5. The stress increases to 0.9 MPa at $t = 80$ s, but the first crossing of the critical stress level occurs only at $t = 89$ s, because the applied stress is substantially smaller than the σ_c value

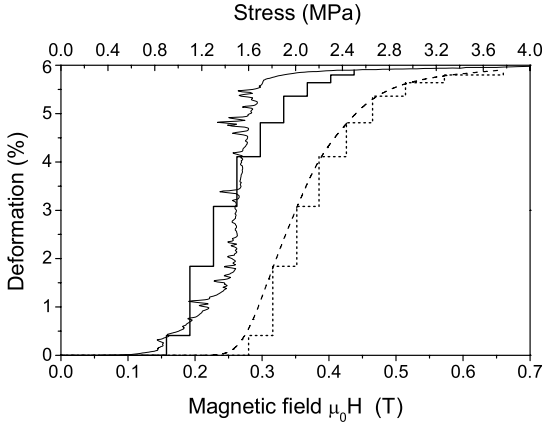

Fig. 3. Deformation vs. stress (solid steps) and deformation vs. field (dashed steps) computed for the case of stepwise stress/field variation. Experimental deformation–stress (solid line) and smoothed deformation–field (dashed line) dependencies are presented for illustration.

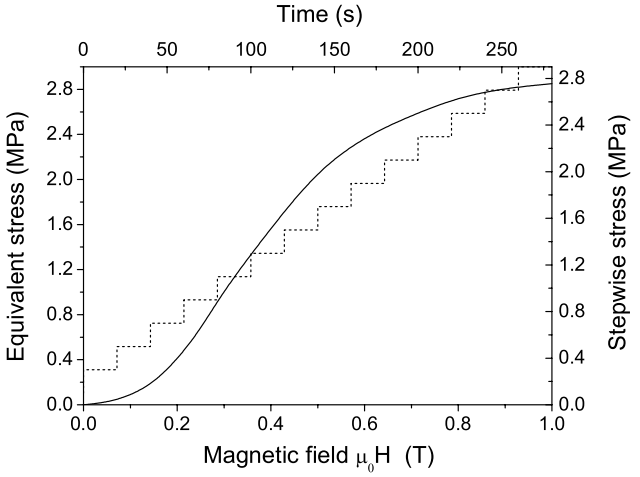

Fig. 2. Stepwise stress vs. time (dashed line) and equivalent stress vs. field (solid line). The equivalent stress derived in Ref. [8] quadratically depends on alloy magnetization value; magnetization vs. field curve has a sigmoidal shape.

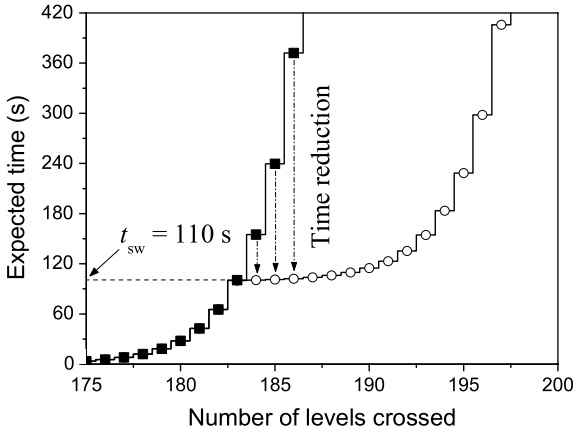

Fig. 4. Expected time vs. the number of critical levels crossed by the fluctuating stress in absence of ultrasound (squares) and with assistance of the ultrasound (open circles). A constant compressive force inducing an axial stress of 1.1 MPa was applied to the twinned martensitic sample in the initial moment.

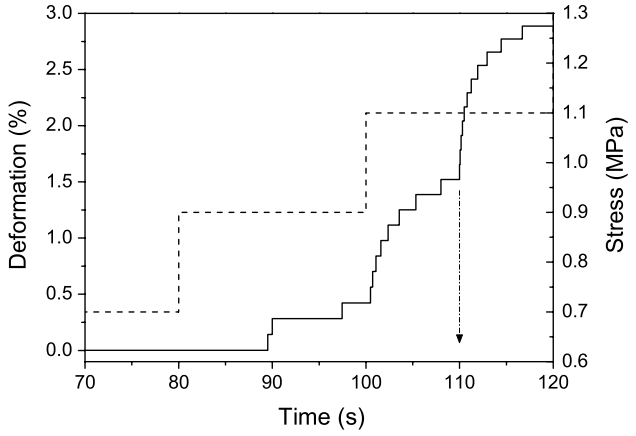

Fig. 5. Time evolution of deformation (solid line) induced by the stepwise stress (dashed line) and ultrasonic oscillations, which were switched on in the moment $t = 110$ s, indicated by vertical arrow. The strain amplitude in the elastic wave ($\varepsilon_A \approx 2 \times 10^{-5}$) corresponds to the oscillatory stress amplitude of 0.25 MPa. Fine steps on the deformation curve correspond to the moments of crossing critical stress levels.

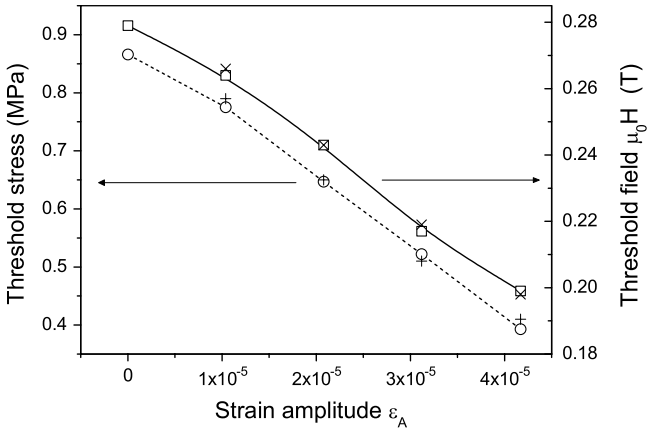

Fig. 7. Threshold field/stress value, which triggers the deformation process, vs. the strain amplitude of the ultrasonic wave: crosses correspond to the values determined from the previous figure, the circles and squares mark the values found by the computation of the expected times (see the text for details).

in Table 1, and therefore a large (and thus low-probability) value of the stress fluctuation is needed to start the deformation process. The next stepwise increase of the stress results in the increase of deformation to 1.5%, and, finally, superposition of ultrasonic oscillations at $t = 110$ s promotes the deformation rise up to 2.9%.

The efficiency of ultrasound as the factor promoting the MID is illustrated in Figs. 6 and 7. According to Fig. 6 the additional deformation induced by the ultrasound with $\varepsilon_A \approx 4 \times 10^{-5}$ (see the curve plotted for $\Delta_+ = 0.5$ MPa) reaches a maximum value ≈2.8% when the field/stress reaches the initial (i.e. observed in the absence of ultrasound) threshold value. Extrapolation of the curves presented in Fig. 6 to zero value of deformation results in the tentative estimation of the threshold field values for the different amplitudes of the ultrasound: $H_{th} \approx 0.20$, 0.22, 0.24 and 0.26 T for the strain amplitudes 4×10^{-5}, 3×10^{-5}, 2×10^{-5} and 10^{-5}, respectively. These threshold

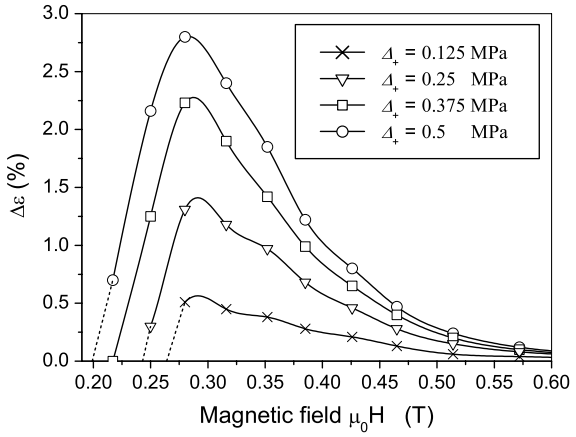

Fig. 6. Additional deformation induced by the ultrasound in presence of magnetic field. The deformation was computed for the stress pulse amplitudes indicated in the legend. These values correspond to the strain amplitudes approximately equal to 10^{-5}, 2×10^{-5}, 3×10^{-5} and 4×10^{-5}.

fields and the appropriate values of the equivalent stress (determined using Fig. 2) are shown in Fig. 7 by crosses. The threshold stress is reduced up to a half of its initial value, the reduction of the threshold field reaches 30%. The changes of the threshold stress and field are different due to the nonlinear character of the equivalent stress function plotted in Fig. 2.

Another way to determine the threshold fields/stresses is based on the direct computation of the expected time values of crossing the critical stress levels. Let k be the order number of the critical stress level defined by the inequalities $\sigma_{k-1} < \sigma_c$, $\sigma_k > \sigma_c$, where σ_c is the threshold value of fluctuating stress introduced in the probability density distribution Eq. (10). In the case of the stepwise stress variation depicted in Fig. 2 the deformation process will start during a time interval (for example, $\Delta t = 20$ s, used in the calculations) of the constant stress level if the fluctuating stress crosses the kth critical level by the end of this time interval, i.e. if $\langle t(k) \rangle = 20$. Average waiting time for crossing the critical level $\langle t(k) \rangle$ depends on the current value of applied stress/field and on the amplitude of the oscillatory stress Δ_+ (see Eqs. (4), (5), (6), (8)). Fig. 8 shows the results of calculations of the average waiting time $\langle t(k) \rangle$ for several steps of increasing applied stress and different values of oscillatory stress amplitude Δ_+. Cross-section of the set of the curves shown in Fig. 8 for different values of oscillatory stress by a horizontal line (which corresponds to a time step $\Delta t = 20$ s) yields the threshold values of quasistatic applied stress to initiate deformation of twinned martensite. These values are indicated by vertical arrows. Data in Fig. 8 demonstrate that the threshold values of stress depend also on the stress variation rate. Indeed, in the case of the stress shown in Fig. 2 the stress variation rate can be changed by changing the time step Δt at constant stress step $\Delta\sigma$. The increase/decrease of this rate corresponds to the parallel translation of the horizontal dashed line in Fig. 8 upwards/downwards and results in the shift of the threshold stresses

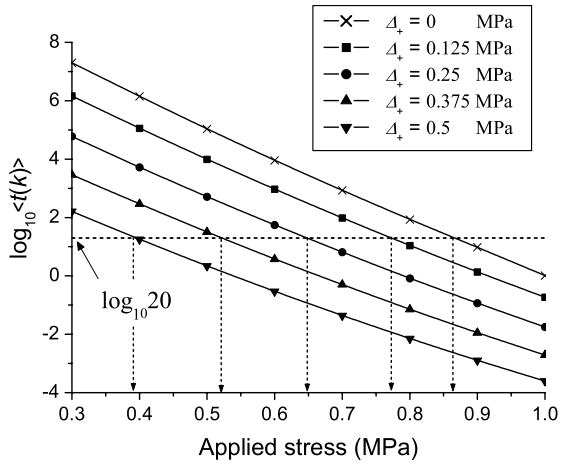

Fig. 8. Average waiting time for crossing the kth critical stress level and start of the deformation of twinned martensite vs. applied stress for different values of oscillatory stress amplitude $\Delta_{\pm}$. The horizontal dashed line corresponds to the time step Δt of 20 s. Vertical arrows define the threshold values of applied stress to initiate the deformation process.

marked by arrows. The dependence of the threshold stress/field on Δt value is physically obvious, because the longer is the time interval, the higher is the probability of crossing of kth critical level by the total stress, which includes the random component (see Eq. (4)).

The threshold stresses determined from Fig. 8 for time step $\Delta t = 20$ s are presented in Fig. 7 by circles. The threshold fields determined from the graph of the equivalent stress function (Fig. 2) are shown in Fig. 7 by squares. A good agreement with the preliminary estimated values (crosses in Fig. 7) is observed.

Finally, the deformation–field dependence can be modeled. Let the specimen be deformed by the application of a stepwise magnetic field and the oscillations being superimposed at zero field value. In this case the entire deformation process occurs in presence of the ultrasonic wave. The computations show that the ultrasonic wave reduces not only the threshold field, but also the field of saturation of MID (Fig. 9). The computations carried out for realistic value of strain amplitude ε_A show the reduction of both characteristic fields by about 30%.

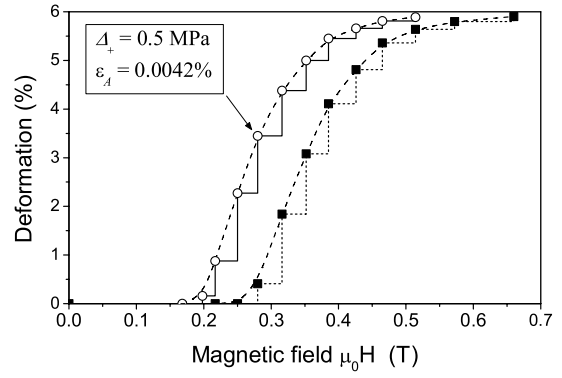

Fig. 9. Deformation vs. field dependence computed for the specimen deformed by stepwise magnetic field in presence of ultrasonic wave (circles, solid steps). The deformation vs. field dependence in the absence of ultrasound is shown for comparison (squares, dashed steps).

4. Summary

1. The modeling of the effect of superimposed mechanical oscillations on the mechanically or magnetically induced deformation of twinned Ni–Mn–Ga martensite shows that the oscillations with realistic values of elastic strain amplitude can appreciably facilitate the deformation process: the superposition of the ultrasound with a strain amplitude of 4×10^{-5} results in a ~30% reduction of the threshold magnetic field and in a ~50% reduction of the threshold stress, which activate the deformation. The magnetic field needed for saturation of the deformation process is also reduced by about 30%. If the field/stress magnitude is close to the threshold value, the additional deformation induced by the ultrasound with the strain amplitude of 4×10^{-5} reaches 2.8%. The strong influence of the ultrasound on the process of superelastic deformation can be understood from the following simplified example: the ultrasound with a strain amplitude of 4×10^{-5} produces in the specimen an axial stress of around 0.5 MPa; superposition of this stress to the threshold stress of about 0.8 MPa shift the total stress to the value, which approximately corresponds to the center of the plateau in the stress–deformation curve, thus producing the deformation close to a half of the saturation value.
2. Due to the random nature of thermal stress, the effect of the ultrasonic oscillations on the mechanically or magnetically induced deformation of twinned Ni–Mn–Ga martensite depends on the speed of the deformation process and duration of exposure to the oscillations. In addition to the points 1 and 2, which were explicitly illustrated by computations, some factors, which can enhance the effect of superposition of oscillations on the deformation process, should be discussed.
   (i) A possible transient process emerging in the moment of superposition of oscillations onto stress/magnetic field should be mentioned. This process can be included in the model as a factor intensifying the thermal stress fluctuations during a period of time of about L/s_t after switching on the oscillations.
   (ii) The dissipation of ultrasonic energy, leading to the heating of the specimen, should be considered in future studies. Heating of the specimen not only increases the average energy of random oscillations of crystal lattice, but also shifts the temperature of the specimen to the reverse martensitic transformation temperature, and therefore, results in the softening of shear elastic modulus and in the appropriate reduction of the threshold stress value. The thermal effect of ultrasound is related to energy dissipation and can be especially important in the following cases:

- for rather high strain amplitudes, since the energy dissipated in a cycle of oscillations, $\Delta W = Q^{-1} E \varepsilon_A^2/4$, where Q^{-1} is the internal friction, which is proportional to the square of elastic strain amplitude;
- for rather high frequencies, since the power dissipated in the sample is proportional to the frequency of oscillations.

In summary, it may be remarked that: (i) the effects modeled in the present paper and the additional factors, which can enhance these effects, are the promising subjects for future experimental studies; (ii) establishing the interrelation between the macroscopic/averaged parameters, which are involved in the present model and those traditionally used for the description of magnetically induced deformation of martensite, on the one hand, and the values used in the microscopic theories (see, e.g., Ref. [20]), on the other hand, is a challenging theoretical problem.

Acknowledgements

V.A.L. is grateful to UIB for financial support during his stay at Departament de Física. Partial financial support from DGI, project MAT2005-00093 is also acknowledged.

References

[1] Ullakko K, Huang JK, Kantner C, O'Handley RC, Kokorin VV. J Appl Phys 1996;69:1966.
[2] O'Handley RC, Murray SJ, Marioni M, Nembach H, Allen MS. J Appl Phys 2000;87:4712–7.
[3] Jiang C, Liang T, Xu H, Zhang M, Wu G. Appl Phys Lett 2002;81:2818–20.
[4] Müllner P, Chernenko VA, Kostorz G. Scripta Mater 2003;49:129–33.
[5] Seguí C, Chernenko VA, Pons J, Cesari E, Khovailo V, Takagi T. Acta Mater 2005;53:111–20.
[6] Vasil'ev AN, Buchel'nikov VD, Takagi T, et al. Physics-Uspekhi 2003;46(6):559.
[7] Kiang J, Tong L. JMMM 2005;292:394–412.
[8] Chernenko VA, L'vov VA, Mullner P, Kostorz G, Takagi T. Phys Rev B 2004;69:134410-1–8.
[9] Heczko O, Straka L. J Appl Phys 2003;94:7139–43.
[10] Müllner P, Chernenko VA, Kostorz G. Scripta Mater 2003;49:129–33.
[11] Brugger D, Kohl M, Hollenbach U, Kapp A, Stiller C. Int J Appl Electromag Mech 2006;23:107–12.
[12] Brugger D, Kohl M, Krevet B. Int J Appl Electromag Mech 2006;23:99–105.
[13] Peterson BW, Feuchtwanger J, Chambers JM, Bono D, Hall SR, Allen SM, et al. J Appl Phys 2004;95:6963–4.
[14] Henry CP, Bono D, Feuchtwanger J, Allen SM, O'Handley RC. J Appl Phys 2002;91:7810–1.
[15] Chernenko VA, L'vov VA, Cesari E. JMMM 1999;196–197:859–60.
[16] Sapozhnikov K, Golyandin S, Kustov S, Van Humbeeck J, De Batist R. Acta Mater 2000;48:1141–51.
[17] Sapozhnikov KV, Vetrov VV, Pulnev SA, Kustov SB. Scripta Mater 1996;34:1543–8.
[18] Lebedev AB. Sov Phys Solid State (Fizika Tverdogo Tela) 1993;35:2305–41.
[19] Freidrich R, Kaiser G, Pechhold W. Metallkd 1969;60:390;
Endo T, Suzuki K, Ishikawa M. Trans Japan Inst Metal 1979;20:706–12;
Kozlov AV, Selitser SI. Mat Sci Eng A 1988;102:143–9;
Tanibayashi M. Phys Stat Sol (a) 1991;128:83–94.
[20] Langeneker B, Jones VO, Illievich J. In: Crawford AH, editor. Proceedings of the 1st International Symposium on High Power Ultrasonics. England: Guildford; 1972. p. 83;
Ohgaku T, Takeuchi N. Phys Stat Sol A 1988;105:153–9.
[21] Paul DI, O'Handley RC, Peterson B. J Appl Phys 2005;97:312–3.
[22] Glavatska NI, Rudenko AA, Glavatskiy IN, L'vov VA. JMMM 2003;265:142–51.
[23] L'vov V, Rudenko O, Glavatska N. Phys Rev B 2005;71:02442-1–6.
[24] Glavatska N, L'vov VA, Glavatskyy I. JMMM 2007;309:244–50.
[25] Kokorin VV, Martynov VV, Chernenko VA. Scripta Met Mater 1992;26:175–7.
[26] Dai L, Cullen J, Wuttig M. J Appl Phys 2004;95:6957–9.
[27] L'vov VA, Glavatska N, Glavatskiy I, Ge Y, Heczko O, Söderberg O, et al. Int J Appl Electromag Mech 2006;23:75–9.
[28] Likhachev AA, Ulakko K. Eur Phys J B 2000;14:263–7.